Hindawi Publishing Corporation
Journal of Nanomaterials
Volume 2008, Article ID 106970, 14 pages
doi:10.1155/2008/106970

Review Article

Nanostructured Mesoporous Silicas for Bone Tissue Regeneration

Isabel Izquierdo-Barba,[1,2] Montserrat Colilla,[1,2] and María Vallet-Regí[1,2]

[1] *Departamento de Química Inorgánica y Bioinorgánica, Facultad de Farmacia, Universidad Complutense de Madrid, 28040 Madrid, Spain*
[2] *Centro de Investigacion Biomédica en Red en Bioingenieria, Biomateriales y Nanomedicina (CIBER-BBN), Spain*

Correspondence should be addressed to María Vallet-Regí, vallet@farm.ucm.es

Received 12 May 2008; Accepted 5 September 2008

Recommended by Michael Harris

The research on the development of new biomaterials that promote bone tissue regeneration is receiving great interest by the biomedical scientific community. Recent advances in nanotechnology have allowed the design of materials with nanostructure similar to that of natural bone. These materials can promote new bone formation by inducing the formation of nanocrystalline apatites analogous to the mineral phase of natural bone onto their surfaces, i.e. they are bioactive. They also stimulate osteoblast proliferation and differentiation and, therefore, accelerate the healing processes. Silica-based ordered mesoporous materials are excellent candidates to be used as third generation bioceramics that enable the adsorption and local control release of biological active agents that promote bone regeneration. This local delivery capability together with the bioactive behavior of mesoporous silicas opens up promising expectations in the bioclinical field. In this review, the last advances in nanochemistry aimed at designing and tailoring the chemical and textural properties of mesoporous silicas for biomedical applications are described. The recent developed strategies to synthesize bioactive glasses with ordered mesopore arrangements are also summarized. Finally, a deep discussion about the influence of the textural parameters and organic modification of mesoporous silicas on molecules adsorption and controlled release is performed.

1. INTRODUCTION

Currently, the biomedical scientificcommunity is demanding new advances in the design ofthird generation bioceramics for bone tissue regenerationtechnologies [1]. Themain goal consists in tailoring bone grafts that mimic as much as possible natural bone tissue biomineralization processes. This involves the growth of nanocrystalline carbonate hydroxyapatites similar to the biological ones onto the materials surfaces, that is, bioactive behavior. Moreover, these biomaterials should stimulate osteoblasts adhesion, proliferation, and differentiation to reduce the postoperative periods [1–6].

Natural hard tissues in vertebrates are natural composite materials, composed of an organic matrix and an array of inorganic nanoapatites. The inorganic phase consists of nanocrystalline apatites with average length of 50 nm, width of 25 nm, and thickness of 2–5 nm [7]. Such inorganic phase is located into an organic matrix mainly consisting of type I collagen [8, 9]. The type I collagen molecules are bonded forming linear chains that are in turn arranged in fibers, giving rise to various macroscopic structures and leaving small empty interstitial compartments where needle-like apatite nanocrystals are deposited during a controled biomineralization process. The integration of both organic and inorganic phases at the nanometric scale modulates the mechanical properties of each kind of bone. The physiological formation mechanism of biological nanocrystalline nanoapatites proposed by Brown [10, 11] involves the growth of biological apatites from two metastables intermediates. Thus, according to the model proposed by Brown for in vivo conditions, the first compound formed onto the bioactive material surface consists in amorphous calcium phosphate which is subsequently transformed into octacalcium phosphate and, finally, the hydrolysis step leads to the formation of a nanocrystalline calcium deficient carbonate

hydroxyapatite [12, 13]. Bone is a dynamic tissue that is constantly being formed and resorbed and this remodeling process is mainly governed by osteoblasts and osteoclasts cells [14, 15]. Osteoblasts govern bone formation processes whereas osteoclasts modulate bone resorption phases and both processes are controled by mechanical and hormonal stimuli. Skeletal tissues display different arrangement and porosity to maintain bone performance, including mechanical, biological, and chemical functions, such as mechanical support, protection of essential body organs, and storage of mineral ions, mostly calcium and phosphate. Bone has a hierarchical organization at many levels of scale which is essential to allow an appropriate physiological performance [16, 17]. Therefore, pore sizes in cortical bone range from 1 μm to 100 μm, being 200 μm to 400 μm in trabecular bone. Moreover, trabecular bone shows 50–95% of porosity, where 55–70% of such pores are interconnected.

The efforts committed to develop bioceramics that could promote new bone formation began in 1971 when Hench reported on the first bioactive composition [18]. Bioactive materials exhibit highly reactive surfaces that are able to bond to living tissues through the formation of nanocrystalline calcium deficient carbonate hydroxyapatites similar to the biological ones. The newly formed apatite, together with the adsorption of biological moieties, constitutes an excellent layer for the action of osteoblasts and the subsequent bone-implant fixation. During the last decades, the development of bioactive materials has allowed important advances in the fields of bone and dental grafting for hard tissue replacement [19–21]. However, the new trends go further than just ensuring the implant-bone fixation. Therefore, bone tissue engineering is a new interdisciplinary research field that emerged because of the excellent potential of certain materials to repair diseased or damaged tissue via regeneration rather than replacement. Such interdisciplinary research area is mainly based on the design of 3D-scaffolds made of biocompatible and bioactive materials that incorporate biologically active agents (drugs, cell, gens, and proteins) to stimulate bone tissue regeneration [22, 23]. 3D-scaffolds will play a significant role in bone tissue regeneration by preserving tissue volume, providing temporary mechanical function, locally delivering biologically active agents, and allowing regenerated tissues to assume their function as scaffold degrades [24]. Thus, one of the main challenges for the scientific community is the development of scaffolds with 3D interconnected porosity and with pores similar in size and number to those existing in natural bone. The size range of these pores is quite wide (1–1000 μm) and at the moment there is a lack of consensus regarding the ideal porosity necessary for bone in growth [25].

Up to date, several porous bioceramics, such as calcium phosphates, glasses, cements, or different biphasic combinations exhibiting open texture and high surface area and porosity, have been reported as excellent candidates to be used as local carriers for local controled delivery systems [1, 26, 27]. Recently, supramolecular chemistry has allowed the emergence of a new generation of advanced bioceramics which exhibit fascinating properties for regenerative purposes. Among such bioceramics, ordered mesoporous materials show potential features to be used as starting materials for the subsequent design and fabrication of scaffolds for bone tissue engineering purposes. These materials exhibit enhanced bioactive capability, and a very precise control over loading and controled release of biologically active agents can be achieved (see Figure 1). This review deals with the recent nanotechnological advances aimed at tailoring the structural, textural, and chemical properties of nanostructured ordered mesoporous silicas with biomedical purposes. To reach this goal, two main aspects concerning mesoporous silicas will be tackled: (i) bioactive behavior and (ii) capability of loading and releasing biologically active molecules in a sustained fashion. Such properties will be described and critically analyzed on the basis of their textural and structural properties and on their composition and the possibility of undergoing organic modification.

2. SILICA-BASED ORDERED MESOPOROUS MATERIALS

Since the discovery of silica-based ordered mesoporous materials in the early 1990s by scientists of the Mobil Corporation [28] and Waseda University [29], these materials have attracted enormous interest. Such nanostructured mesoporous materials have been widely employed in catalysis as host matrices of several guest molecules. Recently, the potential applications of mesoporous silicas as molecule carriers have been expanded into the biomedical field for bone tissue regeneration purposes [3].

Silica-based mesoporous materials constitute a new generation of materials that show ordered arrangements of channels and cavities of different geometry built up from SiO_2 units [30]. These materials exhibit variable pore sizes (2–50 nm), high surface areas (*ca.* 1000 m^2/g), high pore volumes (*ca.* 1 cm^3/g), and homogeneous nanostructures, which can be tailored by varying the synthesis procedure [31]. The synthesis of silica-based ordered mesoporous materials is based on the formation of liquid crystalline mesophases of amphiphilic molecules (surfactant) that serve as template for the in situ polymerization of orthosilicic acid [32]. Well-known examples are MCM-41 and MCM-48 materials, which are synthesized by using cationic surfactants under basic conditions. These mesoporous matrices exhibit pore sizes of *ca.* 2.5 nm and different pore arrangements: 2D-hexagonal (*p6mm* plain group) for MCM-41 and 3D-bicontinuos cubic (*Ia–3d* space group) for MCM-48 [32, 33]. On the contrary, the employment of nonionic surfactants and acid conditions lead to an increase in the pore wall thickness and to an enlargement of the pore size (*ca.* 10 nm) of the resulting mesoporous matrices [34]. SBA-15 [35] and FDU-5 [36] materials constitute two representative examples of such mesoporous materials. SBA-15 exhibits 2D-hexagonal structure with micropores interconnecting adjacent mesopores and FDU-5 presents a 3D-bicontinuos cubic structure similar to that of MCM-48.

It was in 2001, owing to their outstanding adsorptive properties, when mesoporous silicas were proposed for the first time as drug delivery system and ibuprofen, a common anti-inflammatory, was loaded into the pore channels of

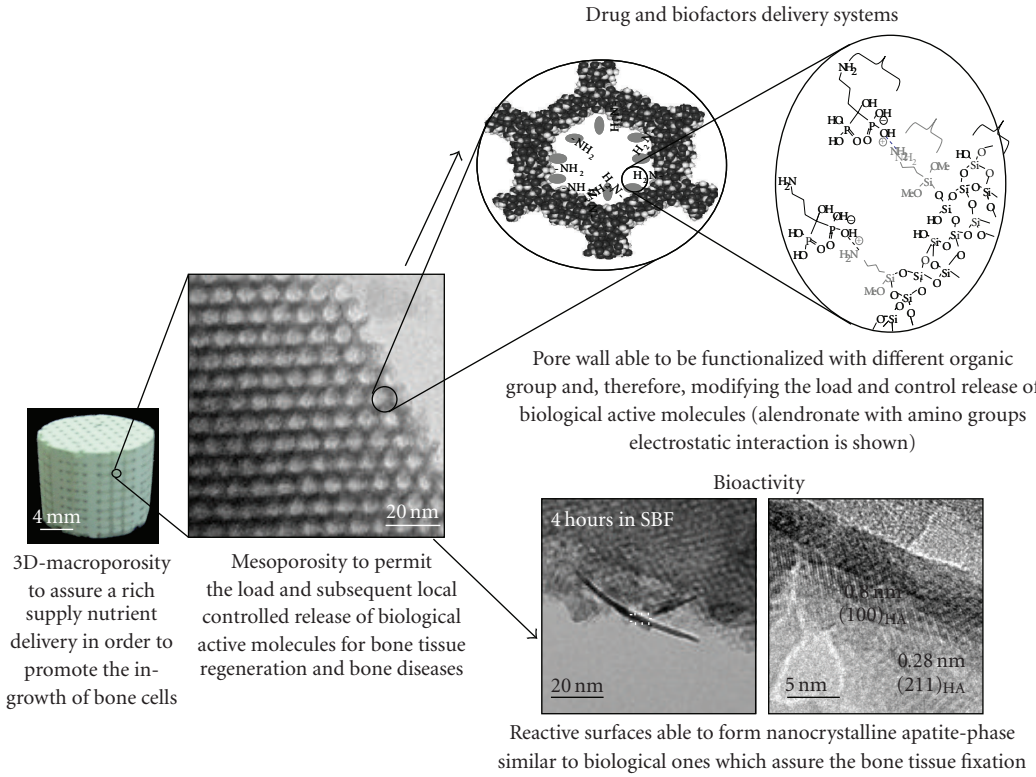

Figure 1: Schematic illustration of functional scaffold based on ordered mesoporous silica for bone regeneration with hierarchically meso- and macroporosity and its corresponding functionality.

MCM-41 and subsequently released in a sustained manner [37]. Since then, this research field has experienced a significant growth and much effort has been devoted to tailor the nanostructure and textural properties (i.e., pore diameter, surface area, and pore volume) of mesoporous materials that allow to achieve a better control over molecule loading and controled release. All the parameters that govern the adsorption and release kinetics of biologically active molecules, with special emphasis on the organic functionalization of the silica walls, will be tackled in this review.

Moreover, the bioactive behavior of silica-based ordered mesoporous materials is undoubtedly an added value when considering these materials for bone tissue regeneration technologies. The combination of both properties, that is, bioactivity and controled delivery capability, is a remarkable synergy that makes mesoporous silicas excellent candidates to be used as starting materials for the manufacture of 3D-scaffolds for bone tissue engineering [38]. The different chemical strategies developed to accelerate the bioactive response of silica-based ordered mesoporous materials will be also discussed in this manuscript.

2.1. *Bioactivity of silica-based ordered mesoporous materials*

Silica-based mesoporous materials are characterized by exhibiting high surface areas and highsurface density of silanol groups (Si–OH). It is well known that silanol groups, which are present in conventional bioactive glasses, are able to react with physiological fluids to produce nanometer-sized carbonated apatites [21, 39]. Therefore, nanostructured silica-based ordered mesoporous materials, which present high amounts of silanol groups covering their surfaces, are expected to induce bioactive responses. It was in 2006 when several in vitro bioactivity assays were performed by soaking three mesoporous materials, SBA-15, MCM-48, and MCM-41, into simulated body fluid (SBF) [40]. The obtained results revealed that SBA-15 and MCM-48 developed a nanocrystalline carbonate hydroxyapatite layer onto their surfaces after 30 and 60 days, respectively. On the contrary, no evidence of formation of an apatite-like layer was observed onto the MCM-41 surface. The different bioactive behavior of SBA-15, MCM-48, and MCM-41 matrices is related to the concentration of silanol groups, and also to the textural and structural properties of the mesoporous matrices. In this case, MCM-41 showed lower concentration of silanol groups (*c.a.* 2×10^{-3} mmol SiOH$\cdot$m^{-2}) than SBA-15 and MCM-48 (*c.a.* 13×10^{-3} mmol SiOH$\cdot$m^{-2}), which could explain the absence of bioactivity in MCM-41 after 60 days. In addition, the textural and structural properties also contribute to the bioactive behavior, since large and accessible pores systems favor the ionic diffusion into the mesoporous framework and consequently the apatite formation is accelerated. Hence, SBA-15, which shows pore size around 9 nm and 3D-pores system with interconnected microporosity, and MCM-48, with 3D-cubic pores system exhibited bioactive response. On the contrary, MCM-41,

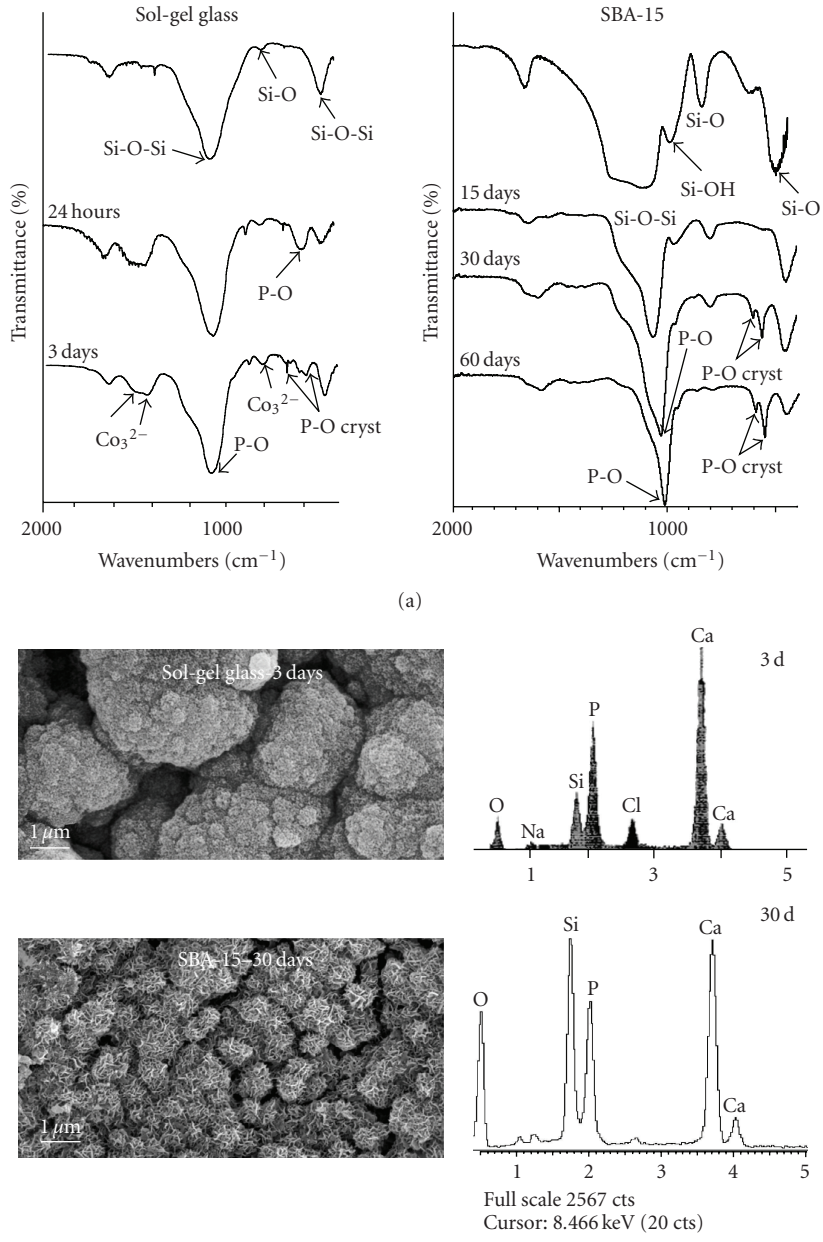

Figure 2: Bioactivity study comparing a conventional sol-gel glass in the SiO_2-CaO-P_2O_5 system and SBA-15 mesoporous material. (a) FTIR study corresponding to the surface of both materials before and after several times soaked in simulated body fluid (SBF). (b) SEM and EDS studies corresponding to the surface of both materials after 3 and 30 days in SBF, respectively.

which presents 2D-pores system with pore sizes close to 2.5 nm did not show bioactive behavior after 60 days of assay. In fact, traditional pure silica mesoporous materials such as SBA-15 and MCM-48 showed bioactive behavior, but the rate of formation of the hydroxyapatite layer is too slow (30–60 days) compared to that of conventional sol-gel bioactive glasses (3 days). Figure 2 displays the bioactivity studies using Fourier transform infraredspectroscopy (FTIR) and scanning electron microscopy-energy dispersive spectroscopy (SEM-EDS) techniques of a conventional sol-gel glass in the system SiO_2-CaO-P_2O_5 versus SBA-15 mesoporous matrix. The results indicated that the band at 600 cm^{-1}, which corresponds to amorphous calcium phosphate, began to split into a doublet at 560–600 cm^{-1} after 3 days in the case of conventional sol-gel glass and after 30 days in the case of SBA-15. Moreover, SEM-EDS studies revealed the formation of spherical agglomerate of particles consisting of needle-like crystals with a Ca/P ratio of 1.5 onto the materials surfaces after different periods of time, confirming the formation of a calcium-deficient nanocrystalline apatite layer.

These findings suggest that high surface areas and porosities are not enough conditions to achieve satisfactory

biomimetic behavior. Consequently, different chemical strategies have been achieved to promote the bioactive response of silica-based mesoporous materials and, therefore to accelerate their bioactive kinetics. Some approaches consisted in the incorporation of P_2O_5 units into the silica mesoporous network [41] or the addition of small amount of bioactive sol-gel glasses [42]. However, the real advance has been to synthesize SiO_2-CaO-P_2O_5 sol-gel glasses with the outstanding textural properties (surface area of 195–427 $(m^2 \cdot g^{-1})$ and pore volume of 0.46–0.61 $cm^3 \cdot g$) and ordered porous arrangements of silica-based mesoporous materials [43, 44]. In this sense, the synthesis of ordered mesoporous glasses was carried out employing the evaporation-induced self-assembly (EISA) method [45]. The synthesis involved the use of a nonionic triblock copolymer surfactant ($EO_{20}PO_{70}EO_{20}$) as structure-directing agent and the employment of tetraethyl orthosilicate (TEOS), triethyl phosphate (TEP), and calcium nitrate, $Ca(NO_3)_2 \cdot 4H_2O$ as SiO_2, P_2O_5, and CaO sources, respectively. The textural and structural properties of this new family of mesoporous glasses can be controled by changing the CaO content of mesoporous glasses. A progressive evolution from 2D-hexagonal to 3D-bicontinuous cubic structure (see Figure 3) with an increase in the textural properties was observed when decreasing the CaO content [46]. The possibility of tailoring both structural and textural features of mesoporous glasses is undoubtedly an attractive advance towards the development of biomaterials that is able to fulfill the essential requirements for specific biomedical applications.

It has been evidenced that this new family of mesoporous glasses exhibits enhanced bioactive behavior, with even faster apatite phase formation than conventional bioactive sol-gel glasses. Besides, it has been revealed that the kinetics of apatite formation in mesoporous glasses is governed by their textural and structural properties, differing from conventional bioactive glasses, where the formation kinetics depended on compositional and textural properties. In this sense, the bicontinuous network in 3D-cubic mesoporous glass with low CaO content (10% in mol), which exhibits high accessibility to the diffusion process in pore systems, has led to the most accelerated bioactive response reported up to date [46]. Transmission electron microscopy (TEM) studies revealed that the formation of the crystalline apatite formation took place after only 4 hours of assay (see Figure 4). Their bioactive response was faster than mesoporous glasses with higher CaO content and 2D-hexagonal structure. Moreover, Figure 4 also shows the Ca^{2+} concentration and pH evolutions in SBF as a function of soaking time. It should be highlighted that there was not a significant increase in calcium and pH, which remained almost constant exhibiting values of 7.45 and 100 ppm, respectively [46]. This is a very important factor to avoid the cytotoxic effect that high local pH values could produce in living tissues. On the other hand, mesoporous glasses with 2D-hexagonal pore arrangements and high CaO content (37% in mol) provided a biomimetic mechanism where a sequential transition from amorphous calcium phosphate (ACP) to octacalcium phosphate (OCP) and to calcium deficient carbonate hydroxyapatite (CDHA) maturation, similar to the in vivo bone biomineralization process, was observed by TEM (see Figure 5) [47]. Such ACP-OCP-CDHA maturation sequence had never been observed before in any other bioactive ceramic. In this case, the open channel array and the textural parameters of 2D-hexagonal structure together with high CaO content allow an intense Ca^{2+}–H_3O^+ exchange that results in local acid pH values that favor the OCP phase formation.

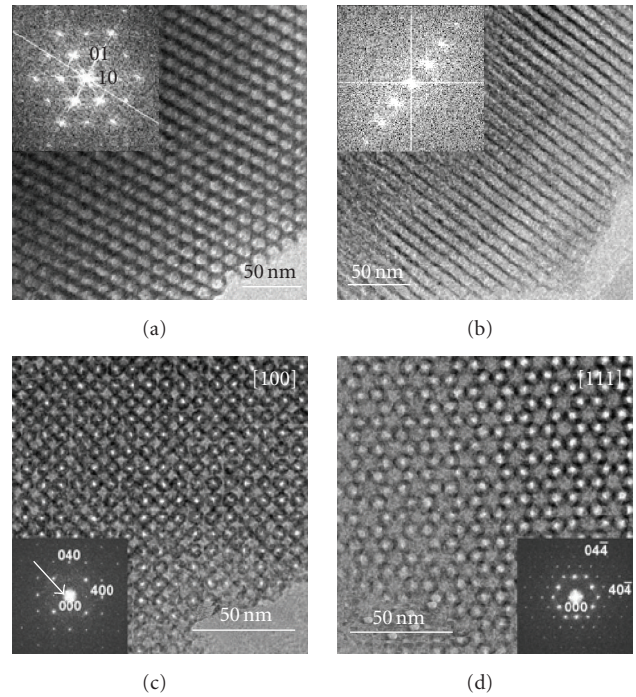

Figure 3: TEM images and their corresponding FT diffractograms of mesoporous glasses in the SiO_2-CaO-P_2O_5 system with different CaO amounts. (a), (b) TEM images taken with the electron beam parallel and perpendicular to the pore channels of a 2D hexagonal structure corresponding to a mesoporous glass with $58SiO_2$-37%CaO-5%P_2O_5 composition; (c), (d) TEM images taken in the 100 and 111 directions of 3D bicontinuous cubic structure with Ia–3d space group corresponding to a mesoporous glass of $85SiO_2$-10%CaO-5%P_2O_5 composition [43].

Therefore, the possibility of tailoring the reactive properties of mesoporous glasses as a function of their textural, structural, and compositional properties allows to obtain materials with high biomimetism-derived biocompatibility. In addition, the fast and intense apatite-phase formation makes mesoporous glasses groundbreaking materials that will probably point out the future guidelines for the synthesis of the next bioactive bioceramics.

2.2. *Silica-based ordered mesoporous materials as controled delivery systems*

Since 2001, when MCM-41 was purposed for the first time as controled delivery system [37], much research effort has been devoted to tailor the chemical properties of mesoporous carriers at the nanometer scale to achieve a better control over loading and release of molecules. The mesoporous carrier is selected according to the features of

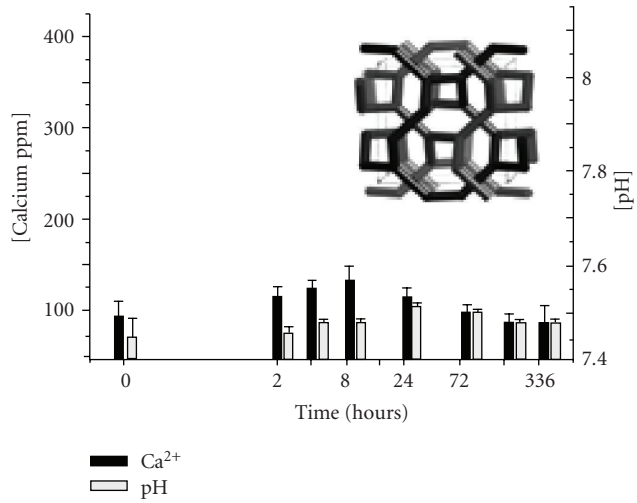

(a)

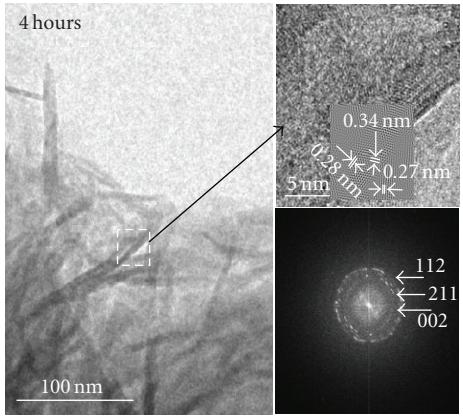

(b)

Figure 4: Bioactive in vitro study corresponding to an ordered mesoporous glass with 3D bicontinuous cubic structure and $85SiO_2$-10%CaO-5%P_2O_5 composition. (Inset) schematic representation of 3D cubic pore arrangement. (a) Variation of calcium content and pH values of SBF after soaking the materials during different periods. (b) HRTEM study corresponding to the surface of mesoporous glasses after 4 hours soaked in SBF. Low magnification image indicates the needle-like crystals formation on the surface of mesoporous glass. Higher magnification and FT transform showing the (002), (211), and (112) reflections corresponding to d-spacings of 0.34, 0.28, and 0.27 nm of an apatite phase.

the guest molecule and the targeted application. Molecule loading is usually performed by impregnation methods by soaking the mesoporous carrier into a concentrated molecule solution. Loading solvent is selected attending to the chemical nature of the guest molecule [48]. Then, the release process is performed by placing the molecule-loaded mesoporous material into SBF solution [49], which exhibits ionic concentrations similar to those in the human plasma, or in physiological serum to make the detection process easy. Therefore, different guest molecules have been successfully confined into mesoporous silicas. Some of these molecules are drugs, such as ibuprofen [37, 50–52], amoxicillin [53], gentamicin [54, 55], erythromycin [51, 56], vancomycin [57], naproxen [58], aspirin [59, 60], diflunisal [58], captopril [61], itraconazole [62], and alendronate [63, 64]. Other guest molecules consisted of biologically active species, such as proteins (bovine serum albumin (BSA) [65–67] and certain amino acids (*L*-tryptophan (*L*-Trp) [68]).

The textural properties (i.e., pore diameter, surface area, and pore volume) of mesoporous materials are key factors that govern molecules adsorption and release [69, 70]. Moreover, functionalization of silica walls using different organic groups has been revealed as the main strategy to modulate molecule loading and release.

2.2.1. *Influence of textural properties*

The textural properties of mesoporous materials (pore diameter, surface area, and pore volume) play an important role in molecule adsorption and release. The influence of all these parameters on performance of controled delivery systems will be discussed in the next sections.

(a) Pore diameter

The adsorption of molecules into mesoporous carriers obeys size selectivity criteria, that is, pore diameter will determine the size of the guest molecule to be hosted. Most of the drugs commonly used in biomedicine are in the range of nanometers. Therefore, they could be easily confined into the pores of nanostructured mesoporous silica. However, pore diameter is a limiting factor when the adsorption of large molecules, such as proteins, is aimed. This is the case of serum albumins, which are one of the major components in plasma proteins. They are involved in several relevant physiological functions of humans and upper mammals, such as binding, transport and delivery of biologically active molecules, including drugs, to specific places in the body [71]. Serum albumins are usually composed of single chains of 582 amino acids and exhibit average length of 10 nm and width of 6 nm [72, 73]. The adsorption of globular proteins, such as bovine serum albumin (BSA) onto MCM-41 matrices, which exhibits pore diameters in the 2–5 nm range, has been reported [74, 75]. The small diameter of MCM-41 impeded the confinement of the protein into the mesopores and consequently, the protein was adsorbed on the outer surface of the mesoporous carrier.

These results evidenced that when the confinement of large size proteins into mesoporous channels is targeted, large pore matrices are needed. Our research group recently applied an improved method to increase the pore diameter of SBA-15 and BSA adsorption and release tests were performed [67]. The increase in the mesopore diameter was achieved by increasing the time of hydrothermal treatment during the mesoporous synthesis, as described elsewhere [76, 77]. The pore diameter of the resulting SBA-15 materials ranged from 8.2 to 11.4 nm employing hydrothermal treatments ranging from 1 to 7 days, respectively. BSA loading tests revealed that there was a direct dependence of protein adsorption on pore size, that is, the greater the pore diameter, the higher the amount of protein loaded. Therefore, conventional SBA-15,

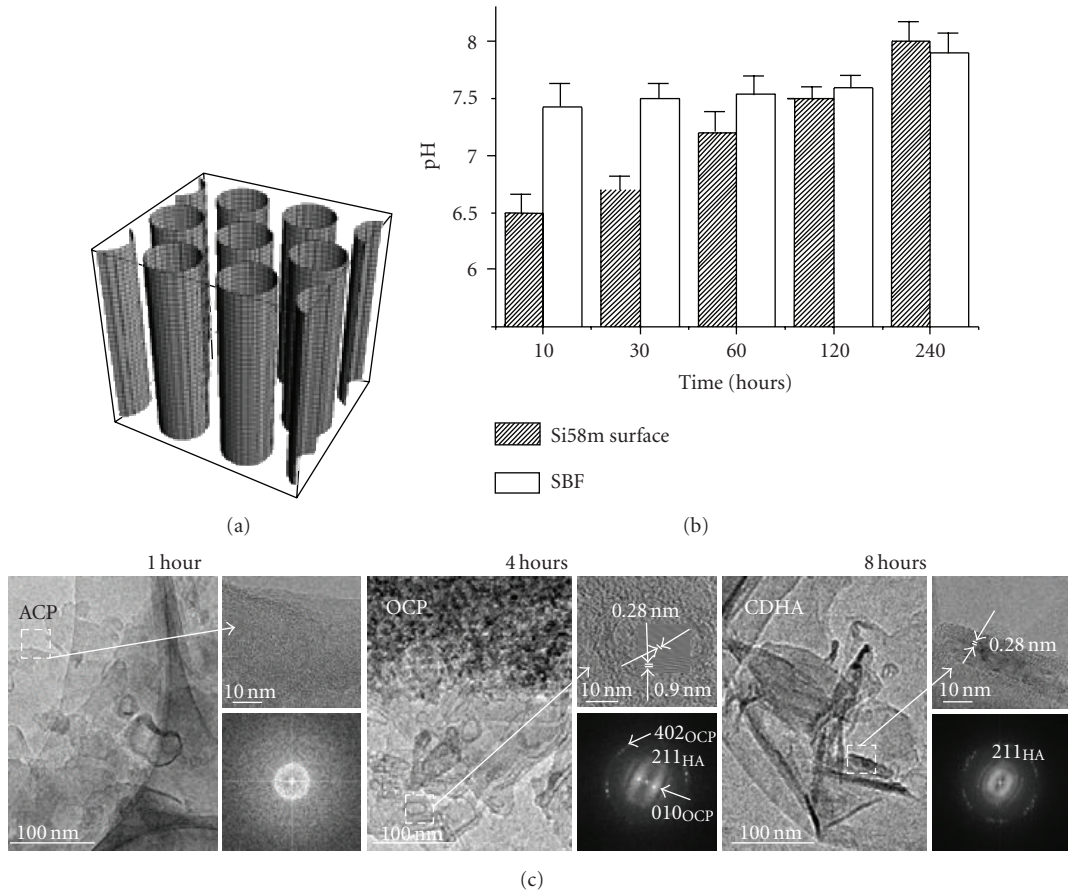

Figure 5: Bioactive in vitro study corresponding to an ordered mesoporous glass with 2D hexagonal structure and $58SiO_2$-37%CaO-5%P_2O_5 composition. (a) Schematic representation of 2D hexagonal pore arrangement. (b) Variation of pH as a function of time at the bioceramic surface and SBF, highlighting the pH range where OCP phase is more stable. (c) HRTEM study after different times of incubation showing a sequential transition from ACP to OCP and to CDHA. For each time, a low magnification image, a higher magnification and its corresponding FT transform are shown.

which presented pore sizes of 8.2 nm, loaded 151 mg/g of BSA. The amount of BSA loaded increased to 234 mg/g, 242 mg/g, and 270 mg/g for mesoporous SBA-15 materials with pore sizes of 9.5 nm, 10.5 nm, and 11.4 nm, respectively (see Figure 6.a.1). In vitro delivery tests were carried out by soaking disc-shaped mesoporous matrices in saline solution (NaCl 0.9%, pH 7.4). Release patterns exhibited and initial burst profile where more than 90% of the adsorbed protein was quickly released during the first 24 hours, followed by a sustained release and the complete delivery was achieved after 192 hours of assay in all tested samples.

Pore diameter has been revealed as a critical factor that modulates release rate of molecules to the delivery medium. This fact was firstly evidenced when MCM-41 materials exhibiting different pore sizes ranging from 2.5 to 3.6 nm were synthesized using cationic surfactants with different length alkyl chains [78]. Ibuprofen, a common anti-inflammatory, was selected and release tests were carried out in a simulated body fluid (pH 7.4) [49]. The resulting release profiles, which are displayed in Figure 6.a.2, revealed that release kinetics strongly depended on mesopore size. Thus, the amount of ibuprofen released to the delivery medium diminished as the pore size decreased from 3.6 to 2.5 nm, evidencing that drug dosage can be modulated depending on the mesopore size.

(b) Surface area

The adsorption of molecules into mesoporous matrices depends on the adsorptive properties of thesilica surface. Therefore, the chemical interactions between the silanol groups covering the silica surface and the functional groups of the guest molecule will determine the amount of molecule loaded. Surface area of mesoporous matrix is the textural parameter that points to the silica surface susceptible to interact with the guest molecule and, consequently, it is expected that the higher the surface area, the higher the amount of molecule loaded. This fact was confirmed when several MCM-41 matrices with different surface areas were employed as ibuprofen delivery systems [78]. MCM-41 mesoporous materials exhibiting surface areas of 768, 936, 1087, and 1157 m^2/g loaded 110, 190, 230, and 340 mg/g of ibuprofen, respectively, evidencing the increase in the drug loading with the surface area increase.

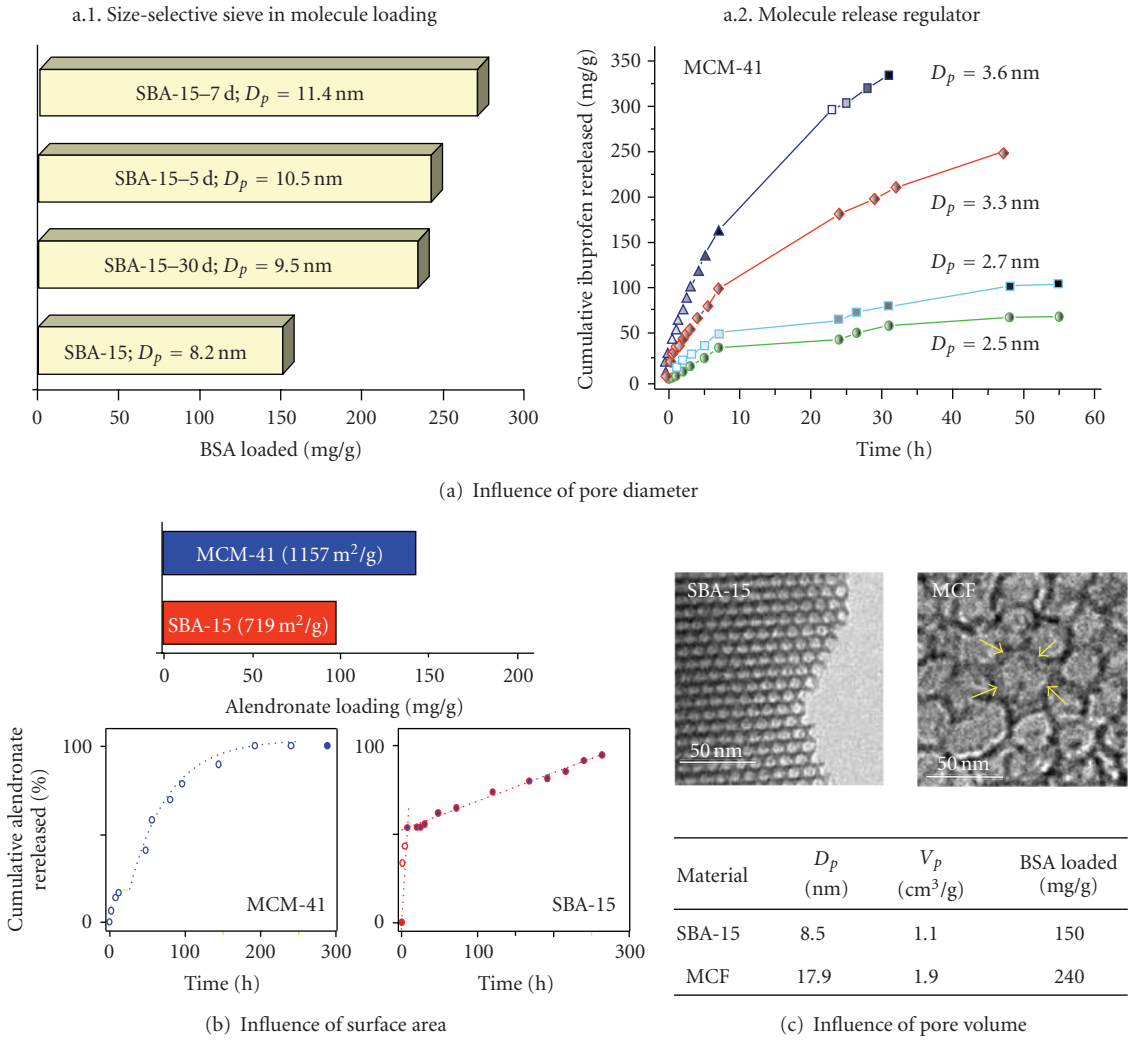

Material	D_p (nm)	V_p (cm^3/g)	BSA loaded (mg/g)
SBA-15	8.5	1.1	150
MCF	17.9	1.9	240

Figure 6: Influence of textural properties. (a) Pore diameter, (b) surface area, and (c) pore volume, on molecule adsorption and release.

With the aim of further establishing the effect of surface area on molecule adsorption, two mesoporous materials, MCM-41 and SBA-15, which exhibit the same structure (2D-hexagonal, *p6mm* symmetry) but different surface areas (1157 m^2/g for MCM-41 and 719 m^2/g for SBA-15) were tested as alendronate delivery systems [63]. Alendronate is a potent bisphosphonate commonly employed for osteoporosis treatments that inhibits bone resorption by osteoclasts and it is a promising drug to be locally applied in bone implant technologies. As displayed in Figure 6(b), the amount of alendronate loaded into MCM-41 (139 mg/g) was higher than that into SBA-15 (83 mg/g), confirming the dependence of drug loading on surface area. Release profiles from both mesoporous carriers into the delivery medium (NaCl 0.9%, pH 7.4) exhibited an initial burst effect when *ca.* 20% and *ca.* 50% of alendronate loaded were quickly released from MCM-41 and SBA-15, respectively (see Figure 6(b)). Afterwards, alendronate was released to the delivery medium in a sustained manner, following first-order kinetics for MCM-41 and zero-order or linear kinetics for SBA-15 materials.

(c) Pore volume

As previously mentioned, the adsorption of molecules into mesoporous matrices is a surface-molecule interaction [79]. For this reason, pore diameter, as the size-selectivity limiting factor, and surface area are key parameters that control the adsorption of molecules. However, when the confinement of really large molecules is targeted, the pore volume available to host the guest molecule plays also an important role in molecules adsorption.

Recently, mesostructured cellular foams (MCFs) have been tested as host matrices for the adsorption of several enzymes and proteins [80, 81]. The synthesis of MCF materials was carried out by using triblock copolymers as surfactants and introducing a swelling agent, commonly trimethylbenzene, into the structure directing template solution [82, 83]. TEM image of SBA-15 (see Figure 6(c)) revealed the presence of two-dimensional hexagonal arrays of pores, typical of hexagonally ordered mesoporous materials with pore sizes of *ca.* 8 nm. In the case of MCF, spherical cells of *ca.* 28 nm with windows of *ca.* 18 nm were observed

(see arrows in Figure 6(c)). These matrices seem suitable to be used as delivery systems of large-size molecules, such as proteins. The amount of BSA loaded was higher in MCF (240 mg/g) than in SBA-15 (150 mg/g), following the same trend than pore volume, being 1.9 cm^3/g and 1.1 cm^3/g for MCF and SBA-15, respectively (see table inset Figure 6(c)). This results evidence that pore volume is an important parameter to consider when aiming at confining large-size and large-volume molecules. However, the effect of other parameters, such as pore diameter into protein loading cannot be overruled. The pore size of SBA-15 is just on the limit of BSA dimensions, which could complicate the protein adsorption into the mesopores. However, such steric hindrance would not take place when MCF, with a pore opening of 18 nm, is used as host matrix.

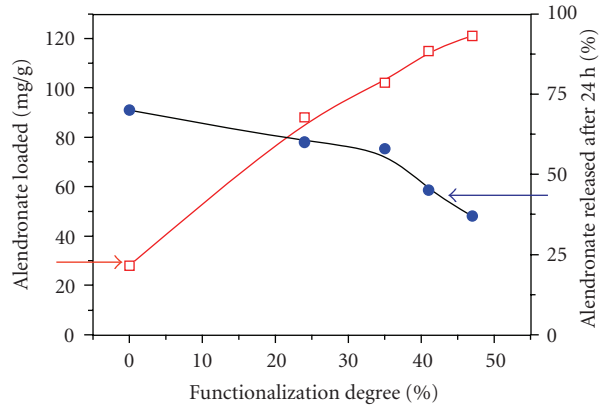

Figure 7: Amount of alendronate loaded and percentage of alendronate released as a function of functionalization degree.

2.2.2. *Influence of organic functionalization*

A straightforward way to optimize the performance of mesoporous matrices as controled delivery systems consists in organically modifying the mesoporous silica walls with appropriate functional groups [69, 70]. On the surface of silica walls, there is a high surface density of silanol groups that can experience organic modification by covalently anchoring organic silanes, $(RO)_3SiR'$ [84]. The adsorption and release of molecules can be effectively controled by using the adequate organic functionalization. To reach this goal, two main strategies have been widely employed. The first one involves the use of organic groups that promote attracting host-guest interactions with the functional groups of the guest molecule. The choice of the functional group would depend on the targeted molecule. For instance, ibuprofen delivery tests from MCM-41 functionalized with several organic groups (chloropropyl, phenyl, benzyl, mercaptopropyl, cyanopropyl, and butyl) revealed that polar groups induced greater ibuprofen adsorption than nonpolar groups [85]. The second strategy concerns the functionalization of mesoporous silica walls using hydrophobic species. In the next sections, some relevant results regarding functionalization using amino groups and functionalization employing hydrophobic groups will be described.

(a) Functionalization using amino groups

Functionalization using amino groups has been a widely employed strategy to attain a better control over molecule loading and release. Therefore, amino functionalized MCM-41 and SBA-15 mesoporous matrices have been tested as alendronate delivery systems [63]. The obtained results indicated that the amount of drug loaded into amino-modified materials was almost 3 fold that of unmodified matrices. This fact could be explained by the stronger attracting interactions taking place between phosphonate groups in alendronate and amino groups of functionalized matrices compared to the weaker interactions through hydrogen bonds between phosphonate groups and silanol groups of unmodified materials. Therefore, amino-modified MCM-41-NH_2 loaded more alendronate (366 mg/g) than unmodified MCM-41 (139 mg/g). Also, amino-modified SBA-15-NH_2 matrix loaded more amount of drug (220 mg/g) than unmodified SBA-15 (83 mg/g). Moreover, drug release assays revealed that amino functionalization of mesoporous silica allowed a better control on the drug release. Thus, the amount of alendronate released after 24 hours was 28% and 58% of the total amount loaded for amino-modified and unmodified MCM-41, respectively. In the case of SBA-15, the 11% and 56% of the total alendronate loaded were released from amino-modified and unmodified materials, respectively, after 24 hours of assay.

Recently, the amino modification of SBA-15 mesoporous materials using different functionalization degrees has been revealed as key factor to modulate alendronate dosage [64]. The amino-modification method was improved by adding a catalyst during the functionalization process. Alendronate loading as a function of experimental functionalization degree is displayed in Figure 7. The amount of alendronate loaded linearly increased as the functionalization degree increased, ranging from 88 mg/g, for the lowest functionalization degree (0%), to 121 mg/g, for the highest functionalization degree (47%). Moreover, functionalization degree also allowed a better control over alendronate release (see Figure 7), that is, the higher the functionalization degree, the smaller the percentage of alendronate released. This work evidences the possibility of modulating drug dosage by varying the functionalization degree of mesoporous matrix, which is particularly interesting when using bisphosphonates since the high potency of these drugs implies that only small local doses are needed.

The organic modification of mesoporous matrices was observed to control release kinetics of proteins, such as BSA [66, 67]. As previously described, SBA-15 materials exhibiting different pore diameters were obtained by varying the time of hydrothermal treatment during their synthesis. These materials were then modified using amino groups to favor attracting interactions with amide groups of protein. It should be highlighted that organic functionalization always leads to a diminishing of pore diameter and consequently, as BSA size is on the limit of SBA-15 mesopore dimensions, after amino functionalization, the amount of BSA loaded

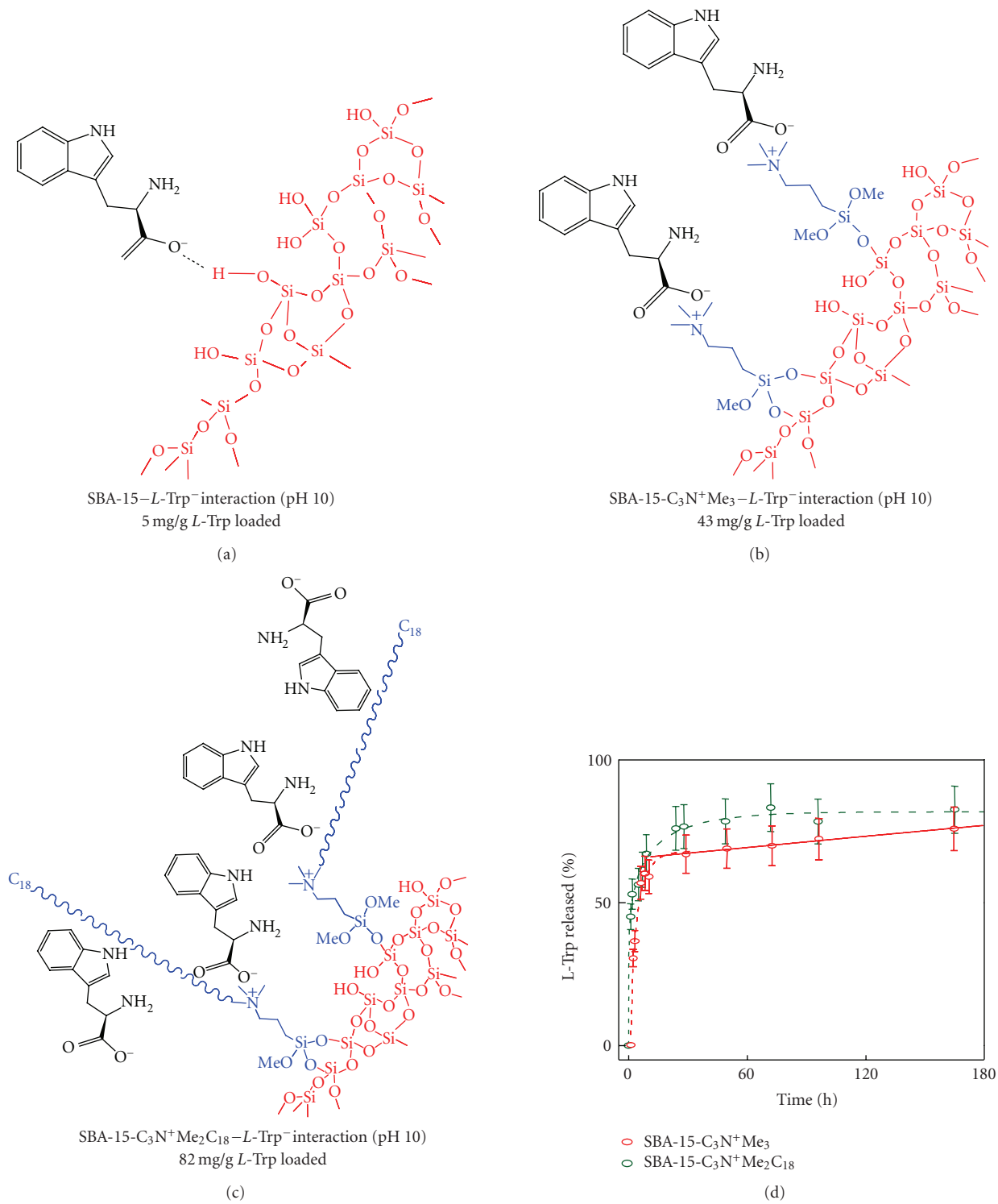

FIGURE 8: Molecular model of interaction between *L*-Trp and (a) unmodified SBA-15, (b) SBA-15 functionalized with short-chain quaternary amines (~$C_3N^+Me_3$), and (c) SBA-15 functionalized with long-chain quaternary amines (~$C_3N^+Me_2C_{18}$). (d) *L*-Trp release profiles from functionalized samples are also displayed.

decreased compared to unmodified materials. However, organic functionalization of SBA-15 had a noticeable effect on BSA kinetic release rate. As a consequence of organic functionalization, the initial burst effect observed in BSA release from unmodified matrices (*ca.* 90%) was drastically reduced after amino modification (*ca.* 30%). Moreover, the release of protein from the mesopores of all amino-modified materials was incomplete, whereas the total amount of

loaded BSA was released after 192 hours from unmodified materials.

Moreover, functionalization of large-pore MCF materials with amino groups has been demonstrated to increase the affinity for BSA [81]. There was an increase in BSA adsorption after amino-modification MCF-NH_2 (270 mg/g) compared to unmodified MCF (240 mg/g), despite of the decrease in pore diameter due to the functionalization. However, amino functionalization has a strong influence on BSA release rate. Unmodified MCF exhibited an initial burst effect when almost 60% of the protein loaded was quickly released to the delivery medium. This burst effect was drastically reduced to *ca.* 10% after amino modification. After 24 hours of assay, 62% of the loaded BSA was released from unmodified MCF material and this percentage decreased to 22% after functionalization with amino groups.

These studies evidence that organic functionalization of silica mesoporous matrices using amino groups allows the control of release kinetics of several molecules that exhibit functional groups able to undergo attracting interaction with amino functions.

(b) Functionalization using hydrophobic groups

The functionalization of mesoporous silica walls with hydrophobic groups is an alternative to control the release of certain molecules. Therefore, SBA-15 mesoporous matrix has been functionalized with different alkyl chains, octyl (C_8) and octadecyl (C_{18}), and erythromycin, a hydrophobic antibiotic was selected to carry out adsorption and delivery assays [56]. As previously commented, organic modification led to a decrease of the effective pore diameter and surface area of SBA-15. The decrease in surface area resulted in diminishing the amount of erythromycin loaded, 130 mg/g and 180 mg/g for SBA-15-C_8 and SBA-15-C_{18}, respectively, compared to unmodified SBA-15 (340 mg/g). Comparable results were reported using mesoporous materials modified by silylation as ibuprofen delivery systems, showing a lower drug loading after silylation [86]. In addition, as a consequence of functionalization with hydrophobic chains, there was a decrease in the wettability of the surface, which made difficult the penetration of the aqueous delivery solution inside the mesopores originating a decrease in the delivery rate. In fact, the erythromycin release rate from SBA-15-C_{18} material was one order of magnitude lower than that from unmodified SBA-15.

Recently, functionalized SBA-15 has been proposed as delivery system of *L*-tryptophan (*L*-Trp) [68], a hydrophobic amino acid present in the three-dimensional structure of many peptides, proteins, and growth factors of interest in bone tissue regeneration technologies [87–89]. *L*-Trp presents an aromatic indol ring that makes necessary to modify the silanol-rich walls of SBA-15. In fact, unmodified SBA-15 loaded less than 5 mg/g of *L*-Trp, probably due to the extremely different chemical nature of hydrophobic amino acid and hydrophilic SBA-15. The small amount of *L*-Trp adsorbed into SBA-15 could be interactions through hydrogen bonds between deprotonated carboxylic group of amino acid and silanol groups covering the silica walls (see Figure 8(a)). For this reason, SBA-15 matrix was organically modified using quaternary amines with different alkyl lengths ($\sim C_3N^+Me_3$ and $\sim C_3N^+Me_2C_{18}$), as illustrated in Figures 8(b) and 8(c) [68]. Functionalization with short alkyl chains ($\sim C_3N^+Me_3$) allowed coulombic attracting interactions between deprotonated carboxylic groups of amino acid ($-COO^-$) and protonated quaternary amines ($-N^+R_4$) covering the mesoporous surface. In this case, the amount of *L*-Trp loaded into SBA-15-$C_3N^+Me_3$ matrix was higher (43 mg/g) than in unmodified SBA-15 (<5 mg/g). On the other hand, using long hydrocarbon chains ($\sim C_3N^+Me_2C_{18}$), two-thirds of the silica surface was functionalized. This high degree of functionalization with hydrophobic chains promoted interaction of mesoporous surface with indol group of *L*-Trp, and consequently, the amount of amino acid loaded increased to 82 mg/g. Moreover, release profiles of amino acid from functionalized SBA-15 materials are displayed in Figure 8(d). In both cases, there is an initial burst effect, where most of the *L*-Trp loaded is quickly released to the delivery medium. After such burst effect, the rest of amino acid is released in a sustained manner, following first-order and zero-order or linear kinetics from SBA-15-$C_3N^+Me_3$ and SBA-15-$C_3N^+Me_2C_{18}$ matrices, respectively.

3. CONCLUSIONS

Nanostructured mesoporous silicas are promising candidates to be used as controled delivery systems of a wide range of biologically active molecules of interest in bone tissue regeneration applications. Recently, much research effort is being dedicated to enhance the bioactive capability of ordered mesoporous silicas. Supramolecular chemistry has allowed the design and synthesis of ordered mesoporous glasses with fascinating textural and structural features that open many paths for the research on high-bioactive nanostructured materials for bone tissue regeneration purposes. These materials have shown high bioactive responses and biomimetic behavior not reported for any bioceramic up to date, which open promising expectations in the biomedical field. Furthermore, much attention has been devoted to tailor the textural properties of nanostructured mesoporous carriers, pore diameter, surface area, and pore volume,with the aim of optimizing their loading capacity depending on the guestmolecule. Moreover, organic modification of mesoporous silica walls brings up many possibilities in molecule adsorption and release by promoting host-guest interactions. The outstanding properties of mesoporous silicas make them suitable to be used as starting materials for the design of scaffolds for bone tissue engineering technologies.

REFERENCES

[1] M. Vallet-Regí, "Ceramics for medical applications," *Journal of the Chemical Society, Dalton Transactions*, no. 2, pp. 97–108, 2001.

[2] L. L. Hench and J. M. Polak, "Third-generation biomedical materials," *Science*, vol. 295, no. 5557, pp. 1014–1017, 2002.

[3] M. Vallet-Regí, "Revisiting ceramics for medical applications," *Dalton Transactions*, no. 44, pp. 5211–5220, 2006.

[4] S. F. Hulbert, "The use of alumina and zirconia in surgical implants," in *An Introduction to Bioceramics*, L. L. Hench and J. Wilson, Eds., pp. 25–40, World Scientific, Singapore, 1993.

[5] D. L. Wise, D. J. Trantolo, D. E. Altobelli, M. J. Yaszemski, J. D. Gresser, and E. R. Schwart, Eds., *Encyclopedic Handbook of Biomaterials and Bioengineering*, Marcel Dekker, New York, NY, USA, 1995.

[6] J. A. Miller, J. D. Talton, and S. Bathia, "Alumina-alumina and alumina-polyethylene total hip prostheses," in *Clinical Performance of Skeletal Prostheses*, L. L. Hench and J. Wilson, Eds., Chapman and Hall, London, UK, 1996.

[7] M. Vallet-Regí and J. M. González-Calbet, "Calcium phosphates as substitution of bone tissues," *Progress in Solid State Chemistry*, vol. 32, no. 1-2, pp. 1–31, 2004.

[8] M. J. Glimcher, "The nature of the mineral phase in bone: biological and clinical implications," in *Metabolic Bone Disease and Clinically Related Disorders*, L. V. Avioli and S. M. Krane, Eds., chapter 2, pp. 23–50, Academic Press, San Diego, Calif, USA, 1998.

[9] D. Eglin, G. Mosser, M.-M. Giraud-Guille, J. Livage, and T. Coradin, "Type I collagen, a versatile liquid crystal biological template for silica structuration from nano- to microscopic scales," *Soft Matter*, vol. 1, no. 2, pp. 129–131, 2005.

[10] W. E. Brown, N. Eidelman, and B. Tomazic, "Octacalcium phosphate as a precursor in biomineral formation," *Advances in Dental Research*, vol. 1, no. 2, pp. 306–313, 1987.

[11] W. E. Brown and M. U. Nylen, "Role of octacalcium phosphate in formation of hard tissues," *Journal of Dental Research*, vol. 43, no. 5, p. 751, 1964.

[12] P. Bodier-Houllé, P. Steuer, J.-C. Voegel, and F. J. G. Cuisinier, "First experimental evidence for human dentine crystal formation involving conversion of octacalcium phosphate to hydroxyapatite," *Acta Crystallographica Section D*, vol. 54, no. 6, pp. 1377–1381, 1998.

[13] G. H. Nancollas and B. Tomazic, "Growth of calcium phosphate on hydroxyapatite crystals: effect of supersaturation and ionic medium," *The Journal of Physical Chemistry*, vol. 78, no. 22, pp. 2218–2225, 1974.

[14] G. H. Nancollas, "In vitro studies of calcim phosphate crystallization," in *Biomineralization. Chemical and Biochemical Perspectives*, S. Mann, J. Webb, and R. J. P. Williams, Eds., chapter 6, VCH, Weinheim, Germany, 1989.

[15] J. E. Davies and M. M. Hosseini, "Histodinamics of endosseous world healing, in bone engineering," in *Bone Engineering*, J. E. Davies, Ed., pp. 1–14, Em Squared, Toronto, Canada, 2000.

[16] S. V. Dorozhkin, "Calcium orthophosphates," *Journal of Materials Science*, vol. 42, no. 4, pp. 1061–1095, 2007.

[17] J. Y. Rho, L. Kuhn-Spearing, and P. Zioupos, "Mechanical properties and the hierarchical structure of bone," *Medical Engineering & Physics*, vol. 20, no. 2, pp. 92–102, 1998.

[18] L. L. Hench, R. J. Splinter, T. K. Greenlee, and W. C. Allen, "Bonding mechanism at the interface of ceramic prosthetic materials," *Journal of Biomedical Materials Research*, vol. 5, no. 6, pp. 117–141, 1971.

[19] L. L. Hench and J. Wilson, "Surface-active biomaterials," *Science*, vol. 226, no. 4675, pp. 630–636, 1984.

[20] L. L. Hench, "Bioactive Glasses and glass ceramics: a perspective," in *Handbook of Bioactive Ceramics*, T. Yamamuro, L. L. Hench, and J. Wilson, Eds., vol. 1, pp. 7–23, CRC Press, Boca Raton, Fla, USA, 1990.

[21] M. Vallet-Regí, C. V. Ragel, and A. J. Salinas, "Glasses with medical applications," *European Journal of Inorganic Chemistry*, vol. 2003, no. 6, pp. 1029–1042, 2003.

[22] S. E. Haynesworth, D. Reuben, and A. I. Caplan, "Cell-based tissue engineering therapies: the influence of whole body physiology," *Advanced Drug Delivery Reviews*, vol. 33, no. 1-2, pp. 3–14, 1998.

[23] J. Bonadio, "Tissue engineering via local gene delivery," *Journal of Molecular Medicine*, vol. 78, no. 6, pp. 303–311, 2000.

[24] S. J. Hollister, "Porous scaffold design for tissue engineering," *Nature Materials*, vol. 4, no. 7, pp. 518–524, 2005.

[25] B. Xie, R. L. Parkhill, W. L. Warren, and J. E. Smay, "Direct writing of three-dimensional polymer scaffolds using colloidal gels," *Advanced Functional Materials*, vol. 16, no. 13, pp. 1685–1693, 2006.

[26] K. A. Hing, S. M. Best, and W. Bonfield, "Characterization of porous hydroxyapatite," *Journal of Materials Science: Materials in Medicine*, vol. 10, no. 3, pp. 135–145, 1999.

[27] M. Colilla, I. Izquierdo-Barba, and M. Vallet-Regí, "Novel biomaterials for drug delivery," *Expert Opinion on Therapeutic Patents*, vol. 18, no. 6, pp. 639–656, 2008.

[28] C. T. Kresge, M. E. Leonowicz, W. J. Roth, J. C. Vartuli, and J. S. Beck, "Ordered mesoporous molecular sieves synthesized by a liquid-crystal template mechanism," *Nature*, vol. 359, no. 6397, pp. 710–712, 1992.

[29] T. Yanagisawa, T. Shimizu, K. Kuroda, and C. Kato, "The preparation of alkyltrimethylammonium-kanemite complexes and their conversion to microporous materials," *Bulletin of the Chemical Society of Japan*, vol. 63, no. 4, pp. 988–992, 1990.

[30] J. Y. Ying, C. P. Mehnert, and M. S. Wong, "Synthesis and applications of supramolecular-templated mesoporous materials," *Angewandte Chemie International Edition*, vol. 38, no. 1-2, pp. 57–77, 1999.

[31] G. J. D. A. A. Soler-Illia, C. Sanchez, B. Lebeau, and J. Patarin, "Chemical strategies to design textured materials: from microporous and mesoporous oxides to nanonetworks and hierarchical structures," *Chemical Reviews*, vol. 102, no. 11, pp. 4093–4138, 2002.

[32] J. S. Beck, J. C. Vartuli, W. J. Roth, et al., "A new family of mesoporous molecular sieves prepared with liquid crystal templates," *Journal of the American Chemical Society*, vol. 114, no. 27, pp. 10834–10843, 1992.

[33] M. Kaneda, T. Tsubakiyama, A. Carlsson, et al., "Structural study of mesoporous MCM-48 and carbon networks synthesized in the spaces of MCM-48 by electron crystallography," *Journal of Physical Chemistry B*, vol. 106, no. 6, pp. 1256–1266, 2002.

[34] D. Zhao, J. Feng, Q. Huo, et al., "Triblock copolymer syntheses of mesoporous silica with periodic 50 to 300 angstrom pores," *Science*, vol. 279, no. 5350, pp. 548–552, 1998.

[35] S. Che, K. Lund, T. Tatsumi, et al., "Direct observation of 3D mesoporous structure by scanning electron microscopy (SEM): SBA-15 silica and CMK-5 carbon," *Angewandte Chemie International Edition*, vol. 42, no. 19, pp. 2182–2185, 2003.

[36] Y. Sakamoto, T.-W. Kim, R. Ryoo, and O. Terasaki, "Three-dimensional structure of large-pore mesoporous cubic Ia-3d silica with complementary pores and its carbon replica by electron crystallography," *Angewandte Chemie International Edition*, vol. 43, no. 39, pp. 5231–5234, 2005.

[37] M. Vallet-Regí, A. Rámila, R. P. Del Real, and J. Pérez-Pariente, "A new property of MCM-41: drug delivery system," *Chemistry of Materials*, vol. 13, no. 2, pp. 308–311, 2001.

[38] M. Vallet-Regí, L. Ruiz-González, I. Izquierdo-Barba, and J. M. González-Calbet, "Revisiting silica based ordered mesoporous materials: medical applications," *Journal of Materials Chemistry*, vol. 16, no. 1, pp. 26–31, 2006.

[39] P. Li, C. Ohtsuki, T. Kokubo, et al., "Effects of ions in aqueous media on hydroxyapatite induction by silica gel and its relevance to bioactivity of bioactive glasses and glass-ceramics," *Journal of Applied Biomaterials*, vol. 4, no. 3, pp. 221–229, 1993.

[40] I. Izquierdo-Barba, L. Ruiz-González, J. C. Doadrio, J. M. González-Calbet, and M. Vallet-Regí, "Tissue regeneration: a new property of mesoporous materials," *Solid State Sciences*, vol. 7, no. 8, pp. 983–989, 2005.

[41] M. Vallet-Regí, I. Izquierdo-Barba, A. Rámila, J. Pérez-Pariente, F. Babonneau, and J. M. González-Calbet, "Phosphorous-doped MCM-41 as bioactive material," *Solid State Sciences*, vol. 7, no. 2, pp. 233–237, 2005.

[42] P. Horcajada, A. Rámila, K. Boulahya, J. González-Calbet, and M. Vallet-Regí, "Bioactivity in ordered mesoporous materials," *Solid State Sciences*, vol. 6, no. 11, pp. 1295–1300, 2004.

[43] X. Yan, C. Yu, X. Zhou, J. Tang, and D. Zhao, "Highly ordered mesoporous bioactive glasses with superior in vitro bone-forming bioactivities," *Angewandte Chemie International Edition*, vol. 43, no. 44, pp. 5980–5984, 2004.

[44] X. Yan, X. Huang, C. Yu, et al., "The in-vitro bioactivity of mesoporous bioactive glasses," *Biomaterials*, vol. 27, no. 18, pp. 3396–3403, 2006.

[45] C. J. Brinker, Y. Lu, A. Sellinger, and H. Fan, "Evaporation-induced self-assembly: nanostructures made easy," *Advanced Materials*, vol. 11, no. 7, pp. 579–585, 1999.

[46] A. López-Noriega, D. Arcos, I. Izquierdo-Barba, Y. Sakamoto, O. Terasaki, and M. Vallet-Regí, "Ordered mesoporous bioactive glasses for bone tissue regeneration," *Chemistry of Materials*, vol. 18, no. 13, pp. 3137–3144, 2006.

[47] I. Izquierdo-Barba, D. Arcos, Y. Sakamoto, O. Terasaki, A. López-Noriega, and M. Vallet-Regí, "High-performance mesoporous bioceramics mimicking bone mineralization," *Chemistry of Materials*, vol. 20, no. 9, pp. 3191–3198, 2008.

[48] M. Vallet-Regí, F. Balas, M. Colilla, and M. Manzano, "Drug confinement and delivery in ceramic implants," *Drug Metabolism Letters*, vol. 1, no. 1, pp. 37–40, 2007.

[49] T. Kokubo, H. Kushitani, S. Sakka, T. Kitsugi, and T. Yamamuro, "Solutions able to reproduce in vivo surface-structure changes in bioactive glass-ceramic A-W^3," *Journal of Biomedical Materials Research*, vol. 24, no. 6, pp. 721–734, 1990.

[50] B. Muñoz, A. Rámila, J. Pérez-Pariente, I. Díaz, and M. Vallet-Regí, "MCM-41 organic modification as drug delivery rate regulator," *Chemistry of Materials*, vol. 15, no. 2, pp. 500–503, 2003.

[51] I. Izquierdo-Barba, Á. Martinez, A. L. Doadrio, J. Pérez-Pariente, and M. Vallet-Regí, "Release evaluation of drugs from ordered three-dimensional silica structures," *European Journal of Pharmaceutical Sciences*, vol. 26, no. 5, pp. 365–373, 2005.

[52] M. Manzano, V. Aina, C. O. Areán, et al., "Studies on MCM-41 mesoporous silica for drug delivery: effect of particle morphology and amine functionalization," *Chemical Engineering Journal*, vol. 137, no. 1, pp. 30–37, 2008.

[53] M. Vallet-Regí, J. C. Doadrio, A. L. Doadrio, I. Izquierdo-Barba, and J. Pérez-Pariente, "Hexagonal ordered mesoporous material as a matrix for the controlled release of amoxicillin," *Solid State Ionics*, vol. 172, no. 1–4, pp. 435–439, 2004.

[54] A. L. Doadrio, E. M. B. Sousa, J. C. Doadrio, J. Pérez Pariente, I. Izquierdo-Barba, and M. Vallet-Regí, "Mesoporous SBA-15 HPLC evaluation for controlled gentamicin drug delivery," *Journal of Controlled Release*, vol. 97, no. 1, pp. 125–132, 2004.

[55] J. M. Xue and M. Shi, "PLGA/mesoporous silica hybrid structure for controlled drug release," *Journal of Controlled Release*, vol. 98, no. 2, pp. 209–217, 2004.

[56] J. C. Doadrio, E. M. B. Sousa, I. Izquierdo-Barba, A. L. Doadrio, J. Pérez-Pariente, and M. Vallet-Regí, "Functionalization of mesoporous materials with long alkyl chains as a strategy for controlling drug delivery pattern," *Journal of Materials Chemistry*, vol. 16, no. 5, pp. 462–466, 2006.

[57] Q. Yang, S. Wang, P. Fan, et al., "pH-responsive carrier system based on carboxylic acid modified mesoporous silica and polyelectrolyte for drug delivery," *Chemistry of Materials*, vol. 17, no. 24, pp. 5999–6003, 2005.

[58] G. Cavallaro, P. Pierro, F. S. Palumbo, F. Testa, L. Pasqua, and R. Aiello, "Drug delivery devices based on mesoporous silicate," *Drug Delivery*, vol. 11, no. 1, pp. 41–46, 2004.

[59] W. Zeng, X.-F. Qian, Y.-B. Zhang, J. Yin, and Z.-K. Zhu, "Organic modified mesoporous MCM-41 through solvothermal process as drug delivery system," *Materials Research Bulletin*, vol. 40, no. 5, pp. 766–772, 2005.

[60] Y. Zhu, J. Shi, W. Shen, et al., "Stimuli-responsive controlled drug release from a hollow mesoporous silica sphere/polyelectrolyte multilayer core-shell structure," *Angewandte Chemie International Edition*, vol. 44, no. 32, pp. 5083–5087, 2005.

[61] F. Qu, G. Zhu, S. Huang, et al., "Controlled release of Captopril by regulating the pore size and morphology of ordered mesoporous silica," *Microporous and Mesoporous Materials*, vol. 92, no. 1–3, pp. 1–9, 2006.

[62] R. Mellaerts, R. Mols, J. A. G. Jammaer, et al., "Increasing the oral bioavailability of the poorly water soluble drug itraconazole with ordered mesoporous silica," *European Journal of Pharmaceutics and Biopharmaceutics*, vol. 69, no. 1, pp. 223–230, 2008.

[63] F. Balas, M. Manzano, P. Horcajada, and M. Vallet-Regí, "Confinement and controlled release of bisphosphonates on ordered mesoporous silica-based materials," *Journal of the American Chemical Society*, vol. 128, no. 25, pp. 8116–8117, 2006.

[64] A. Nieto, F. Balas, M. Colilla, M. Manzano, and M. Vallet-Regí, "Functionalization degree of SBA-15 as key factor to modulate sodium alendronate dosage," *Microporous and Mesoporous Materials*, vol. 116, no. 1-3, pp. 4–13, 2008.

[65] H. H. P. Yiu, C. H. Botting, N. P. Botting, and P. A. Wright, "Size selective protein adsorption on thiol-functionalised SBA-15 mesoporous molecular sieve," *Physical Chemistry Chemical Physics*, vol. 3, no. 15, pp. 2983–2985, 2001.

[66] S.-W. Song, K. Hidajat, and S. Kawi, "Functionalized SBA-15 materials as carriers for controlled drug delivery: influence of surface properties on matrix-drug interactions," *Langmuir*, vol. 21, no. 21, pp. 9568–9575, 2005.

[67] M. Vallet-Regí, F. Balas, M. Colilla, and M. Manzano, "Bone-regenerative bioceramic implants with drug and protein controlled delivery capability," *Progress in Solid State Chemistry*, vol. 36, no. 3, pp. 163–191, 2008.

[68] F. Balas, M. Manzano, M. Colilla, and M. Vallet-Regí, "*L*-Trp adsorption into silica mesoporous materials to promote

bone formation," *Acta Biomaterialia*, vol. 4, no. 3, pp. 514–522, 2008.

[69] M. Vallet-Regí, "Ordered mesoporous materials in the context of drug delivery systems and bone tissue engineering," *Chemistry: A European Journal*, vol. 12, no. 23, pp. 5934–5943, 2006.

[70] M. Vallet-Regí, F. Balas, and D. Arcos, "Mesoporous materials for drug delivery," *Angewandte Chemie International Edition*, vol. 46, no. 40, pp. 7548–7558, 2007.

[71] D. C. Carter and J. X. Ho, "Structure of serum albumin," *Advances in Protein Chemistry*, vol. 45, pp. 153–203, 1994.

[72] T. Peters, *All about Albumin: Biochemistry, Genetics and Medical Applications*, Academic Press, San Diego, Calif, USA, 1995.

[73] S. Sugio, A. Kashima, S. Mochizuki, M. Noda, and K. Kobayashi, "Crystal structure of human serum albumin at 2.5 Å resolution," *Protein Engineering*, vol. 12, no. 6, pp. 439–446, 1999.

[74] J. Deere, E. Magner, J. G. Wall, and B. K. Hodnett, "Mechanistic and structural features of protein adsorption onto mesoporous silicates," *Journal of Physical Chemistry B*, vol. 106, no. 29, pp. 7340–7347, 2002.

[75] A. Katiyar, L. Ji, P. G. Smirniotis, and N. G. Pinto, "Adsorption of bovine serum albumin and lysozyme on siliceous MCM-41," *Microporous and Mesoporous Materials*, vol. 80, no. 1–3, pp. 311–320, 2005.

[76] M. Kruk, V. Antochshuk, and M. Jaroniec, "New approach to evaluate pore size distributions and surface areas for hydrophobic mesoporous solids," *Journal of Physical Chemistry B*, vol. 103, no. 48, pp. 10670–10678, 1999.

[77] S. A. El-Safty, T. Hanaoka, and F. Mizukami, "Design of highly stable, ordered cage mesostructured monoliths with controllable pore geometries and sizes," *Chemistry of Materials*, vol. 17, no. 12, pp. 3137–3145, 2005.

[78] P. Horcajada, A. Rámila, J. Pérez-Pariente, and M. Vallet-Regí, "Influence of pore size of MCM-41 matrices on drug delivery rate," *Microporous and Mesoporous Materials*, vol. 68, no. 1–3, pp. 105–109, 2004.

[79] G. Buntkowsky, H. Breitzke, A. Adamczyk, et al., "Structural and dynamical properties of guest molecules confined in mesoporous silica materials revealed by NMR," *Physical Chemistry Chemical Physics*, vol. 9, no. 35, pp. 4843–4853, 2007.

[80] Y.-J. Han, G. D. Stucky, and A. Butler, "Mesoporous silicate sequestration and release of proteins," *Journal of the American Chemical Society*, vol. 121, no. 42, pp. 9897–9898, 1999.

[81] X. Zhang, R.-F. Guan, D.-Q. Wu, and K.-Y. Chan, "Preparation of amino-functionalized mesostructured cellular foams and application as hosts for large biomolecules," *Journal of Materials Science: Materials in Medicine*, vol. 18, no. 5, pp. 877–882, 2007.

[82] P. Schmidt-Winkel, W. W. Lukens Jr., D. Zhao, P. Yang, B. F. Chmelka, and G. D. Stucky, "Mesocellular siliceous foams with uniformly sized cells and windows," *Journal of the American Chemical Society*, vol. 121, no. 1, pp. 254–255, 1999.

[83] P. Schmidt-Winkel, W. W. Lukens Jr., P. Yang, et al., "Microemulsion templating of siliceous mesostructured cellular foams with well-defined ultralarge mesopores," *Chemistry of Materials*, vol. 12, no. 3, pp. 686–696, 2000.

[84] F. Hoffmann, M. Cornelius, J. Morell, and M. Fröba, "Silica-based mesoporous organic-inorganic hybrid materials," *Angewandte Chemie International Edition*, vol. 45, no. 20, pp. 3216–3251, 2006.

[85] P. Horcajada, A. Rámila, G. Férey, and M. Vallet-Regí, "Influence of superficial organic modification of MCM-41 matrices on drug delivery rate," *Solid State Sciences*, vol. 8, no. 10, pp. 1243–1249, 2006.

[86] Q. Tang, Y. Xu, D. Wu, and Y. Sun, "Hydrophobicity-controlled drug delivery system from organic modified mesoporous silica," *Chemistry Letters*, vol. 35, no. 5, pp. 474–475, 2006.

[87] L. J. Suva, G. A. Winslow, R. E. H. Wettenhall, et al., "A parathyroid hormone-related protein implicated in malignant hypercalcemia: cloning and expression," *Science*, vol. 237, no. 4817, pp. 893–896, 1987.

[88] A. Valín, A. García-Ocaña, F. De Miguel, J. L. Sarasa, and P. Esbrit, "Antiproliferative effect of the C-terminal fragments of parathyroid hormone-related protein, PTHrP-(107–111) and (107–139), on osteoblastic osteosarcoma cells," *Journal of Cellular Physiology*, vol. 170, no. 2, pp. 209–215, 1997.

[89] R. M. Cuthbertson, B. E. Kemp, and J. A. Barden, "Structure study of osteostatin PTHrP[Thr107](107–139)," *Biochimica et Biophysica Acta*, vol. 1432, no. 1, pp. 64–72, 1999.